

Numerical simulation of fission product release under accidental conditions with the MFPR code

M.S. Veshchunov^{*1} and R. Dubourg^{*2}

⁽¹⁾ : Nuclear Safety Institute of the Russian Academy of Sciences (IBRAE) Moscow (Russia)

⁽²⁾ : Institut de Radioprotection et de Sûreté Nucléaire, S^tPaul lez-Durance (France)

*corresponding authors : yms@ibrae.ac.ru (095) 955 2232

roland.dubourg@irsn.fr (33) 4 42256513

Abstract – The mechanistic code MFPR developed in collaboration between IRSN (Cadarache, France) and IBRAE (Moscow, Russia) is described. Exhaustive description of gas behaviour in grain and out of grain is given in relation with individual validation results on analytical experiments under various conditions (steady irradiation, transient, post-irradiation annealing). It is shown that microscopic defects in the UO₂ crystal structure can strongly influence fission gases transport out of grains and release from fuel pellets. These defects include point defects, such as vacancies, interstitials and fission atoms and extended defects, such as bubbles, pores and dislocations. The mechanistic behaviour of chemically active elements is also presented. It is based on complex association of diffusion-vaporisation mechanism involving multiphase and multi-component partial thermochemical equilibrium at grain boundary with accurate calculation of fuel oxidation. Examples of application to VERCORS 4 and 5 experiments show the possibilities of the code in the frame of severe accident interpretation

Keywords : UO₂, fission products, fission gases, mechanistic code.

1. Introduction

MFPR code (Module for Fission Product Release), is a mechanistic description of Fission Product behaviour in intact UO₂ fuel under different regimes including irradiation regime, annealing regime, accidental situations (LOCA and severe accidents) (Veshchunov 2003), (Dubourg 2003). Mainly, the code helps in interpreting complex large scale (Dubourg 2004) or semi analytical experiments (Ducros 2001) but it is also used for benchmarking of more simplified reactor code models. Is is fully validated on separate-effect tests, semi-analytical out-of-pile tests and large scale in-pile tests.

An initial version of the code was based on the progenitor code VICTORIA (Heames 1992) which was based, similarly to the FASTGRASS code (Rest 1994), on consideration of equilibrium state of intragranular gas bubbles formed from the solid solution of gas atoms in UO₂ matrix under irradiation conditions. This consideration radically simplifies the theory, since in this case the defect structure of the crystal (including point defects, such as vacancies and interstitials, and extended defects, such as dislocations) is practically excluded from consideration and is well grounded only under steady-state irradiation conditions (with except of high burnups). However, such simple (steady-state) conditions can be relatively well

described by a simple parametric Booth model or other semi-empirical correlation models, so, the advantage of the mechanistic approach is not so visible.

Under transient and/or annealing conditions interactions of bubbles with point defects and dislocations become essential. Lacking mechanistic description of real defects, various artificial mechanisms were introduced in the codes, in order to simulate these complicated regimes. These mechanisms require new "effective" parameters, which introduce strong uncertainties in the code predictions, and, as a result, the advantage of the mechanistic approach is smeared out.

That was one main reason for the code MFPR development, which self-consistently describes evolution of various defects and their interactions with gas atoms and bubbles migrating out of grains. In the code, additional parameters characterizing the crystal defect structure also arise, however, being physically grounded, these new microscopic parameters can be fixed from the analysis of available experimental data, and then used without any artificial tuning in further calculations. .

In addition, as shown by many observations and interpretations, the release of chemically active elements strongly depends on formation of separate phases, mainly at grain boundaries, and thermal behaviour of these phases in various gas atmospheres that determine the fuel oxygen potential and thus the stability of the different phases. The MFPR module includes modelling of chemistry effects on the behaviour of fission products (FP) within irradiated oxide fuel at high temperatures in the interval 500 – 3000 K. The ' $UO_2 - FP - O$ ' system is considered as a as a multiphase system consisting of multi-component phases. Within the fuel matrix the fission products migrate as atoms to the gas bubbles and solid phase precipitates at grain faces, and their mobility depends in particular on the extent of fuel oxidation characterized by the stoichiometry deviation. The release rate is thus proportional to partial pressures of FP vapors determined by chemical states of condensed FP species. In connection with that description, an advanced model for fuel oxidation in steam/air mixtures was developed and implemented in the MFPR code. The major mechanism for release of the fission products is their vaporization on the gas/solid interface.

2. Physical Processes and Models

Due to fission processes, a wide spectrum of fission product (FP) elements is created in the UO_2 matrix, the most important being combined into 15 element groups with the total release 1.87 per fission: *Cs, Ce, I, Eu, Mo, Nd, Ru, Nb, Ba, Sb, Sr, Te, Zr, Xe, La*.

It is assumed that FP elements exist in the UO_2 matrix in atomic form. All impurity atoms formed due to fission processes migrate to grain boundaries. On this way, fission gas atoms can be captured by intragranular gas bubbles, which can also migrate to grain boundaries. Part of the captured atoms can be escaped from bubbles by irradiation-induced and thermal resolution processes.

Chemical interactions between the FP elements and the dissolved oxygen result in formation of separate phases in solid precipitates on the grain boundaries and vaporization to the intergranular gas bubbles. These processes affect significantly the release rates of all FP elements including noble gases.

Intergranular bubbles are classified into three groups: bubbles on grain faces (GF), on grain edges (GE) and in grain corners (GC). The GF bubble growth progresses up to the grain surface saturation, when interlinkage of the GF bubble and formation of grain face channels to the grain edges and corners occurs. Growth of the GE and GC bubbles leads to their

interconnection by tunnels and formation of open porosity.

In the MFPR model, the process of the FP release from solid fuel is divided into two consequent stages:

- intragranular FP transport from the bulk to the grain boundary accompanied by formation of solid precipitates and gaseous species in the intergranular bubbles,
- accumulation of FP-bearing gases in the intergranular bubbles, and release to the open porosity through the system of bubbles on the grain boundaries and the net channels and tunnels.

The model currently ignores the delay in the FP releases into the gap related to the gas transfer both through the channel net and through the open porosity.

2.1. Intragranular Transport of FP Elements

In the transport problem a fuel grain is considered for simplicity as an isotropic sphere. The problem is formulated separately (and in different manners) for two subsystems: the noble gas (Xe , Kr) atoms dissolved in the matrix and filling the grain bubbles, and the atoms of chemically active element and molecules of compounds formed by these elements.

2.1.1. Diffusion and Release of Chemically Active FP Elements

In the MFPR chemistry model, irradiated oxide fuel including fission products and dissolved oxygen is considered as a multiphase system consisting of multi-component phases. Basing on experimental data (Kleykamp 1985) and thermo-chemical calculations (Imoto 1986, Cordfunke 1988, Ball 1989, Cordfunke 1993, Moriyama 1997), the principal phases that appeared in the irradiated UO_2 and considered in the model are the “fuel–FP” solid solution, the metal phase, the oxide phase of complex ternary compounds, the solid phase of CsI and the gas phase.

Zirconium, rare earth and alkaline earth elements are characterized by a high affinity to oxygen. Within UO_2 matrix these elements exist mainly in the form of oxides. Zirconium and rare earth elements characterized by a high affinity to oxygen are partially or completely miscible with uranium dioxide to form a solid solution. Relatively low solubility of barium results in that the majority of barium in the form of uranates, zirconates and molybdates is precipitated as the multi-component 'grey' phase, which also includes ternary compounds of strontium and caesium. Solubility of the metals, Mo and Ru , and their oxides in solid UO_2 is extremely low. These metals (along with Tc , Rh , Pd) are present in the metallic ('white') inclusions of the oxide fuel. Within the fuel matrix the fission products migrate as atoms (Grimmes 1991) to the gas bubbles and condensed precipitates at grain faces, and their mobility depends in particular on the extent of fuel oxidation.

In the current MFPR version it is assumed that separate solid phases (precipitates) are formed on grain faces at the interface with gas bubbles; solid precipitates are in equilibrium with the gas phase and with the solid solution. Partitioning of elements between chemical compounds and phases and the fuel stoichiometry are calculated self-consistently as they are determined by a balance between a series of oxidation/reduction reactions and solid state diffusion.

To formulate the transport problem, the complex system is separated into two subsystems. That is (1) solid solution (SS) of FP elements, their oxides and atomic oxygen dissolved in UO_2 matrix, and (2) the subsystem 'solid precipitates – gas phase' (SP/G) including the metallic, “grey” phases, and the phase of condensed $CsI(c)$. Concentration profiles of FP elements in SS are described by the diffusion equations:

$$\frac{\partial}{\partial t} Y_i^{(1)} = B_i + r^{-2} \frac{\partial}{\partial r} \left(D_i r^2 \frac{\partial}{\partial r} Y_i^{(1)} \right), \quad (1)$$

where $Y_i^{(1)}$ is the local volume concentration of the i -th element in the subsystem 1 – solid solution, B_i is the rate of generation of the i -th element due to fission, D_i is the diffusion coefficient. Boundary conditions for these equations are determined by the thermo-chemical equilibrium within the SP/G subsystem and at the subsystem interface, which in its turn depends on fluxes of elements out of SS. The equilibrium composition of the phases is treated in terms of semi-ideal chemistry model in which phenomenological solid solubilities of FP elements are taken into account, and the chemical potential of dissolved oxygen is described by Lindemer–Besmann correlation [Lindemer 1985].

Solution of the complex problem discussed above yields partitioning of elements between chemical state within the SP/G subsystem and between the two subsystems. The subsequent migration of the FP elements in the form of gaseous compounds to open porosity is related to the intergranular bubble growth kinetics.

2.1.2. Transport of fission gas

In the bi-modal approach similar to that of VICTORIA and FASTGRASS codes, the effects related to a finite width of the bubble size distribution are ignored. The basic space-time dependent variables are the concentrations of gas atoms C_g and bubbles C_b , the average number of gas atoms within a bubble N_b , and the average bubble volume V_b .

Additionally, MFPR includes self-consistent consideration of point defects (vacancies and interstitials) and dislocations, which mutually interacts with each other and with gas bubbles and sintering pores during their evolution under irradiation or annealing conditions. These defects are described by three additional variables: vacancy concentration C_v , interstitial concentration C_i , dislocation density (length per unit volume) ρ_d , and concentration of atoms captured by dislocations Y_d .

Transport equations for C_g and concentration of atoms-in-bubbles $Y_b = N_b C_b$ can be written as:

$$\frac{\partial C_g}{\partial t} = D_g \Delta C_g - F_{g \rightarrow b} - F_{g \rightarrow d} + \kappa G, \quad (3)$$

$$\frac{\partial Y_b}{\partial t} = \nabla (D_b \nabla Y_b) - \omega_{bmg} Y_b + F_{g \rightarrow b} - F_{b \rightarrow d} \quad (4)$$

where:

$$F_{g \rightarrow b} = k_{gg} F_n C_g^2 + k_{gb} (C_g - C_g^{eq}) C_b - b G Y_b, \quad (5)$$

$$k_{xy} \equiv 4\pi (D_x + D_y) (R_x + R_y), \quad x, y = g, b. \quad (6)$$

Different terms in the right hand side of these equations correspond to following physical effects, each being characterized by a particular kinetic parameter:

- Diffusion (D_g and D_b are the diffusivities of gas atoms and bubbles, respectively);
- Gas atom generation by fission (G is the fission rate and $\kappa = 0.241$ is the probability of Xe formation by fission);
- Bubble biased migration (ω_{bmg}) along the temperature gradient;

- Bubble nucleation (with the nucleation rate F_n);
- Gas atom capture by bubbles (R_g is the gas atom radius and R_b is the bubble radius in the capture kernel k_{gb});
- Thermal resolution (C_g^{eq} is the equilibrium gas concentration);
- Radiation induced resolution (b is the resolution probability factor).

Superposition of these effects (along with the Van-der-Waals equation for the gas state) determines, in particular, the intragranular bubbles concentration C_b and mean radius R_b , as well as gas release to the grain faces.

In growing grains, the boundary conditions for Eqs. (3) and (4) are imposed at moving grain boundaries :

$$\left. \frac{\partial C_g}{\partial r} \right|_{r=0} = 0, \quad C_g \Big|_{r=R_{gr}(t)} = C_\delta, \quad \left. \frac{\partial Y_b}{\partial r} \right|_{r=0} = 0, \quad Y_b \Big|_{r=R_{gr}(t)} = 0. \quad (7)$$

Additionally, sweeping of intragranular bubbles by moving grain boundaries takes place. The MFPR model for the grain growth with retarding effect of attached bubbles is presented in Section 2.6.

2.2. Evolution of point defects in irradiated UO₂ fuel

Evolution of the vacancy and interstitial fields in grains is described in the mean field approximation (Brailsford 1981) in terms of dimensionless concentrations, c_v and c_i (number of vacancies and interstitials per uranium atom), by the following equations:

$$\dot{c}_v = -(k_v^2 + k_{vgb}^2)D_v c_v - \alpha D_i c_i c_v + K_e + K_b + K_p + (1 - \xi)K, \quad (8)$$

$$\dot{c}_i = -(k_i^2 + k_{igb}^2)D_i c_i - \alpha D_i c_i c_v - K_d + K, \quad (9)$$

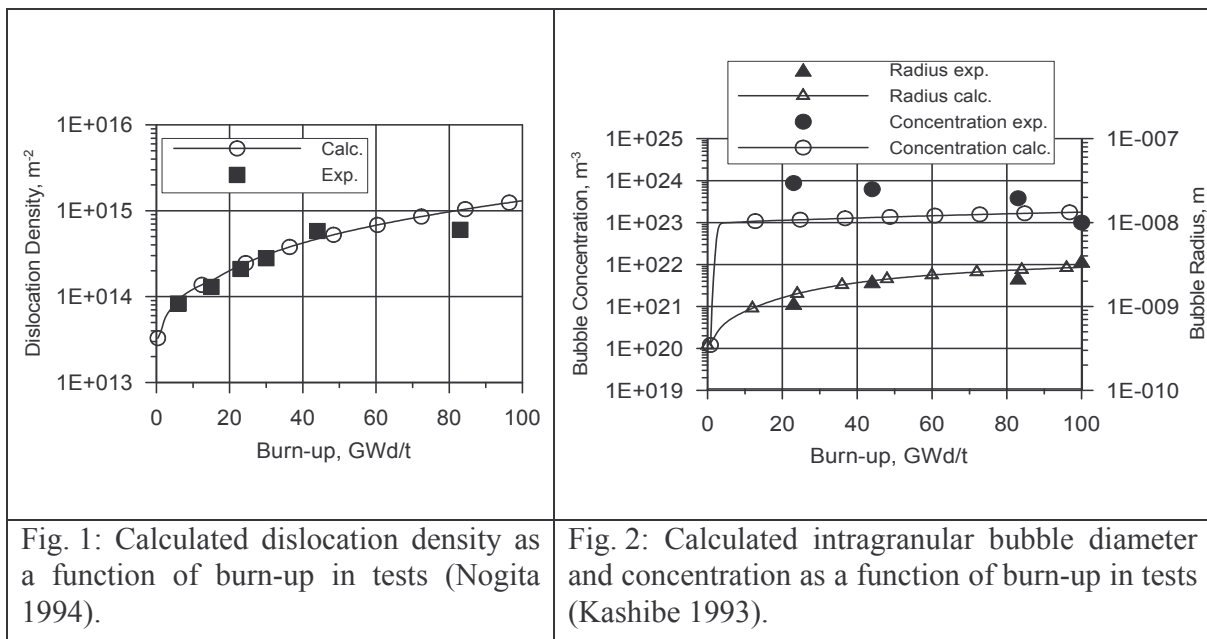
where D_v and D_i are the vacancy and interstitial diffusion coefficients, respectively; α is the recombination constant; k_v^2 and k_i^2 are the total sink strength of vacancies and interstitials into the extended defects (gas bubbles, pores, vacancy clusters and dislocations), respectively; k_{vgb}^2 and k_{igb}^2 are the grain boundary sink strength for vacancies and interstitials, respectively; K is the Frenkel pair production rate (d.p.a. s⁻¹) proportional to the fission rate G ; ξK is the rate at which vacancies are removed from solution to form vacancy loops; K_e is the rate of the vacancy thermal production; K_p is the rate of the vacancy irradiation induced re-solution (knockout) from pores; K_b is the rate of the vacancy irradiation induced re-solution from gas bubbles; K_d is the rate of the interstitial absorption due to the interstitial loop generation (Shestak 2004).

2.3. Evolution of extended defects

Generation of dislocation loops occurs mainly during the initial period of irradiation, concurrently with the fuel densification process, and therefore, may be significantly influenced by the kinetics of pore sintering. For this reason, comparative analysis of existing models for pore evolution under irradiation conditions was performed and the most adequate model is chosen for further development and implementation in MFPR (Shestak 2004). Consequently, in the new MFPR code version both processes of dislocation loops generation and pore shrinkage are considered simultaneously and self-consistently with the point defects and gas bubbles evolution.

Results for the dislocation density evolution obtained by the MFPR code are in a satisfactory agreement with measurements from (Nogita 1994), Fig. 1. In addition, these results provide initial conditions for simulation of annealing regimes, which are rather sensitive to the dislocation density attained during pre-irradiation period of the annealing tests.

Owing to increase of the total sink of vacancies into the extended defects (bubbles and dislocations) in the course of their evolution, a strong reduction of the vacancy concentration at a late stage of irradiation takes place (in accordance with Eq. (8)). In its turn, the bubble nucleation rate is directly proportional to the vacancy concentration (Veshchunov 2000) and thus is strongly suppressed, leading to “saturation” of the bubble concentration observed in recent tests with high burn-up fuel (Kashibe 1993), Fig. 2.



2.4. Intragranular bubbles under annealing conditions

Microstructure observations of irradiated fuel in the annealing tests confirm that gas release is accompanied with a rapid growth of the intragranular bubbles (up to hundreds *nm* at high annealing temperatures) and a noticeable decrease (by several orders of magnitude) of the bubble concentration. This process of the bubble number decrease is usually associated with the Brownian motion of the bubbles leading to their coalescence into larger ones in the grain bulk and transport to the grain boundaries.

During bubbles growth and coalescence extended defects such as dislocation loops uniformly distributed in the grain bulk, may act as the main sources of vacancies (necessary for the bubble equilibration) and afford the equilibrium concentration of the point defects in the crystal bulk. This explains dislocation creep and enhanced bubble growth by dislocation sweeping under annealing conditions, observed in (Whapham 1966).

In this situation a new mechanism for gas release due to dislocation creep emerges (Ozrin 2002). This mechanism considers sweeping of bubbles and delivery them to the grain boundaries by climbing dislocation segments in the course of vacancy generation (necessary for equilibration of growing bubbles).

After some time a strong pinning of dislocations by swept bubbles can saturate this source of point defects, and grain boundaries apparently become the dominant source of vacancies during the subsequent period of the annealing tests. In this situation a vacancy flux directed from grain surface to its interior arises that induces bubble biased migration along the vacancy gradient in the opposite direction, as proposed recently by (Evans 1997) in a qualitative approach.

Simulation of the annealing tests by MFPR shows that the dislocation sources acting in the initial period of annealing stage significantly suppress gas release predicted by the Evans mechanism, and becomes dominant during the initial period. As a result, the dislocation mechanism provides so called “burst release” observed in the initial stage of annealing, whereas the vacancy mechanism (considered by Evans) combined with the advanced model for bubble diffusivity (proposed by (Mikhlin 1979)) provides a more gradual release in a late period of annealing stage (when dislocations become immobile).

Superposition of the above described mechanisms and models allows adequate description of various annealing tests (Zacharie 1998), (Une 1990), as shown in Figs. 3 and 4 (Ozrin 2002). Calculations enable to achieve a good agreement with experimental data for the fractional gas release, Fig. 3, and simultaneously for the value of intragranular bubble size, Fig. 4. Indeed, in the end of annealing stage the mean bubble diameter measured in similar tests (Une 1990) was ≈ 55 nm, whereas calculated diameter is equal to 62 nm. A good agreement with the measured bubbles concentration is also attained in these calculations.

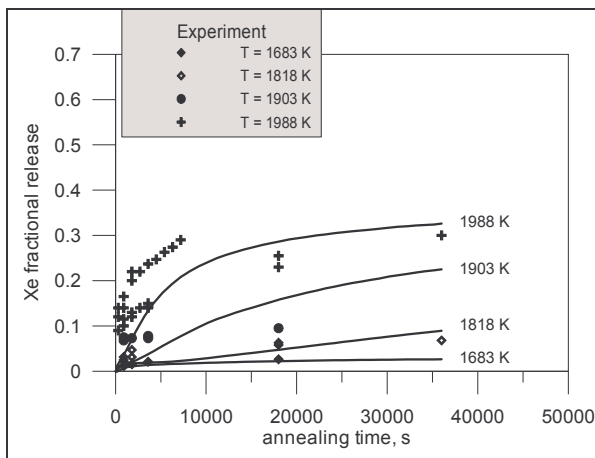


Fig. 3: Calculation results for *Xe* release as a function of annealing time at different temperatures in tests (Zacharie 1998).

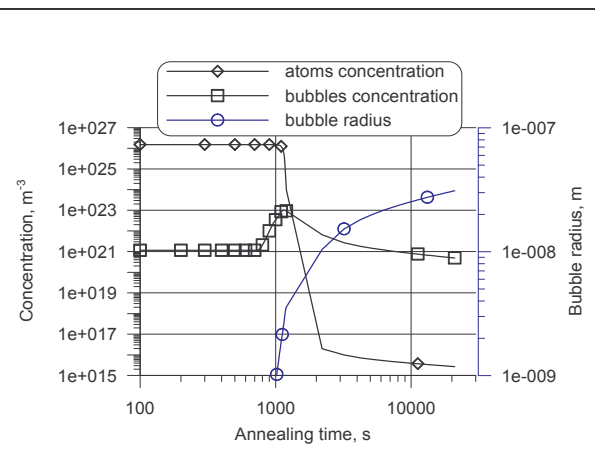


Fig. 4: Calculation results for *Xe* atom and bubble concentrations and bubble radius as functions of annealing time at 1800 °C.

At high annealing temperatures ($\geq 2000^\circ\text{C}$) MFPR predicts an essential decrease of the vacancy concentration in the central region of the grain. This results in a strong over-pressurisation of bubbles so that the thermal re-resolution effect becomes significant. In particular, it reduces sinking of gas atoms into the bubbles and results in additional diffusion flux of gas atoms out of the grain. This high-temperature effect is illustrated by calculation of annealing regime in VI-3 test (Osborne 1992), Fig. 5.

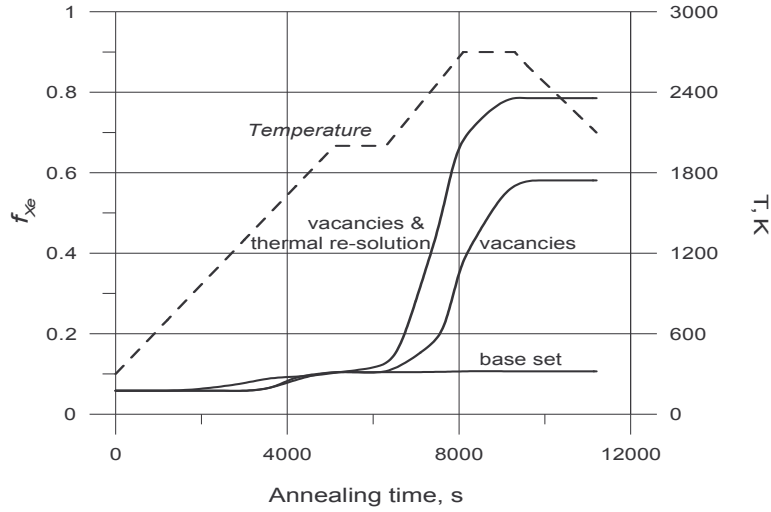


Fig. 5: MFPR simulation of VI-3 test: joint effect of the vacancy and thermal re-solution models after subsequent implementation in the base code.

2.5. Intergranular FP Transport, Release and Swelling Models

The MFPR model for the transport of Xe atoms self-consistently takes into account effects of atom diffusion along the grain surface and irradiation induced re-solution from intergranular bubbles (Veshchunov 2000a, Berdyshev 2002). The “circulation” of gas atoms collected by growing intergranular bubbles from the grain face and then returned back (by the re-solution process) into the grain matrix, makes bubbles much less effective sinks for gas atoms in the course of their growth saturation. In particular, this allows prediction of a noticeable gas release from fuel when the grain face coverage is far below the saturation value $\approx 50\%$ determining onset of grain face bubble interlinking.

The model was validated against the tests (Une 1990) and (Kashibe 1991). In these tests the fractional coverage of grain faces by bubbles was evaluated from SEM photographs as ≈ 6 and 10% (Kashibe 1991), respectively. Significant fractional fission gas release (up to 20–30%) during their base irradiation was measured by pin puncture tests from these specimens without visible bubble interlinking on the grain faces. Results of the model calculations are compared with the measured values in Table 1 and confirm the important conclusion on the onset of gas release at coverages far below the saturation value ($\approx 50\%$).

This conclusion allows application of the new model to analysis of the MOX fuel irradiated in PWR rods, in which fission gas release is relatively high under normal irradiation conditions despite there is no evidence of interconnected intergranular bubbles.

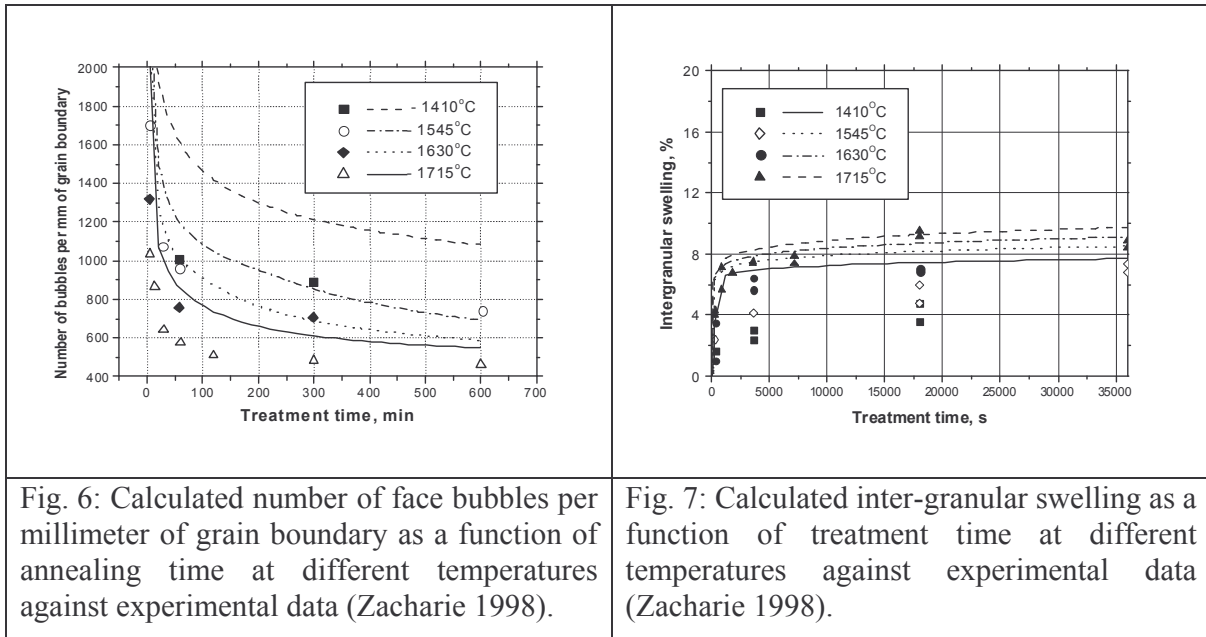
Table 1. Modeling of experiments (Une 1990, Kashibe 1991)

	Face bubble diameter, nm	Fractional coverage, %	Kr release, %
MFPR calculations	216	5.9	10
Experiment	229	6.6–10.1	10–20

Coalescence of face bubbles due to their random migration is considered as the main

mechanism of grain face bubbles relaxation. The model of this phenomenon proposed in (Zacharie 1998) for annealing conditions is refined and extended to the general case of fuel operation conditions (e.g. steady-state irradiation and temperature transients) (Berdyshev 2002), on the base of the general theory (Geguzin 1971) of grain face bubbles migration and coalescence.

Validation of the new model against the fuel grain face microstructure and swelling measurements (Zacharie 1998) allows reasonable agreement of the code predictions with measurements, Figs. 6 and 7.



2.6. Grain Growth Model

A new model for the grain growth in irradiated and non-irradiated UO_2 pellets was recently developed in the MFPR code (Veshchunov 2002). The model is based on the Nichols' analysis (Nichols 1968) of the drag force exerted by attached bubbles and pores on migrating grain boundaries with supplementary consideration of grains coalescence within the Hillert's mean field approach (Hillert 1965). It is shown that the grain growth rate becomes controlled by the movement of the second-phase particles (bubbles, pores) with significantly smaller sizes than predicted by consideration of the stand-alone boundary migration problem, i.e. the retarding effect of attached bubbles was increased in this approach.

Furthermore, the main deficiency of the model inherited from the previous approach associated with consideration of retarding effect using the standard mechanisms of bubble mobility for intragranular bubbles, was removed. Namely, a new mechanism of the lenticular grain face bubble migration which controls the bubble mobility and determines the drag force exerted on the grain boundary was developed.

The model was implemented in the MFPR code and validated against tests (Turnbull 1974) on grain growth in irradiated fuel. In comparison with the previous code version calculations, the new results were in a much better agreement with measurements, Figs. 8 and 9.

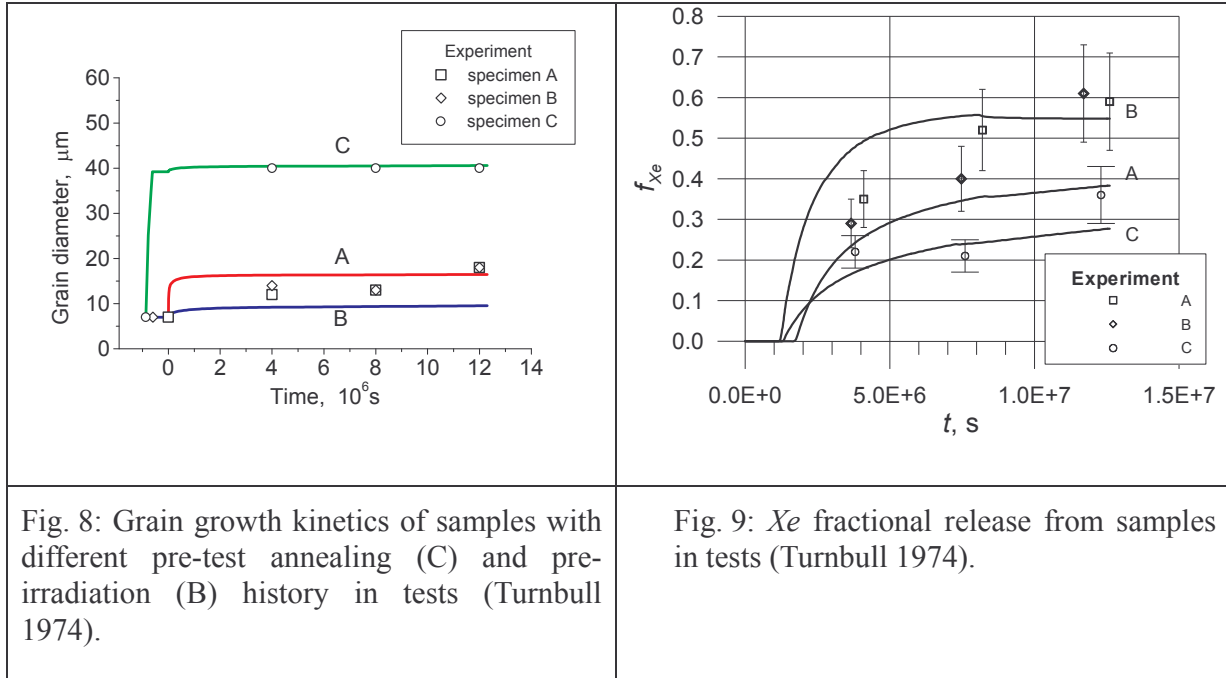


Fig. 8: Grain growth kinetics of samples with different pre-test annealing (C) and pre-irradiation (B) history in tests (Turnbull 1974).

Fig. 9: Xe fractional release from samples in tests (Turnbull 1974).

3. Application to integral tests VERCORS.

The VERCORS program was conducted for IRSN in the LAMA facility in CEA Grenoble (Ducros 2001). It aims to reproduce, in annealing regime, kinetics of fission products (FP) release in different atmospheres and for different burn ups. The most reliable results were obtained in tests VERCORS 4 and 5 which were performed in various atmosphere conditions at high temperature: pure reducing for VERCORS 4 and pure steam for VERCORS 5.

The samples are constituted by three irradiated pellets ($\sim 40\text{GWd/tU}$) in their original cladding and two depleted half pellets placed at the end of the clad. These samples were stored for 10 years, and then re-irradiated at low power in the SILOE facility. The experimental sequence begins within less than 40 hours after re-irradiation.

After intermediate steps at low temperatures (between 700 and 1300 K in He or mixed H_2/H_2O atmosphere) temperature is increased ($1\text{ K}\cdot\text{s}^{-1}$) up to a nearly one hour plateau at intermediate temperature ($\sim 1573\text{ K}$) in a mixed atmosphere (H_2O/H_2 flow molar ratio near 0.85-0.9) to obtain complete clad oxidation. Then, the temperature is increased again to a high temperature plateau maintained half an hour. The main difference between the two experiments is connected with the high temperature plateau in a He/H_2 atmosphere in VERCORS 4 and pure steam atmosphere in VERCORS 5 (this gas phase composition is injected just after the oxidation plateau).

Examples of MFPR results for these experiments on caesium behaviour are given in Figs. 10 and 11, respectively. In both tests the calculated release values are in good agreement with experimental data. It is shown that Cs behaviour is mainly associated with ternary compounds Cs_2UO_4 and Cs_2MoO_4 stability during experiment.

In VERCORS 4, during the clad oxidation plateau ($\sim 6000\text{-}10000\text{s}$), some of the hydrogen produced reacts with the fuel leading to a first step of Cs release due to some Cs_2UO_4

destruction. Then after complete clad oxidation the remaining injected steam interacted with fuel producing some Cs_2MoO_4 . In the final stage of experiment in pure hydrogen atmosphere the remaining part of Cs_2UO_4 was destroyed and Cs_2MoO_4 was unstable, both giving the final release.

In VERCORS 5, a rather identical scheme might be proposed but in this case, with pure steam atmosphere, the transfer from Cs_2UO_4 to Cs_2MoO_4 is quite complete and the first Cs release step (Cs_2UO_4) is followed by vaporisation of the Cs_2MoO_4 near 2300 K which gives the final release.

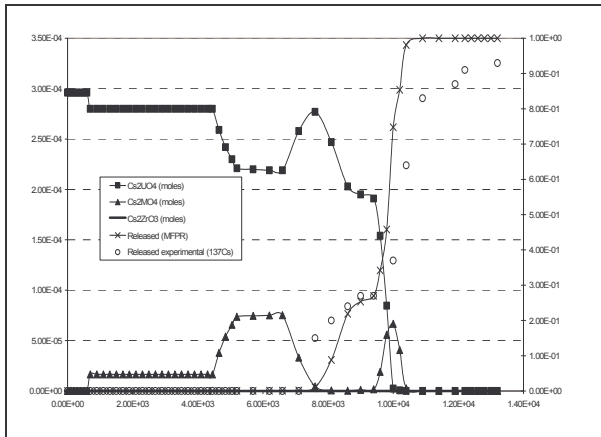


Fig. 10: Calculated Cs behaviour in VERCORS 4 as compared with experimental data (^{137}Cs) (Ducros 2001).

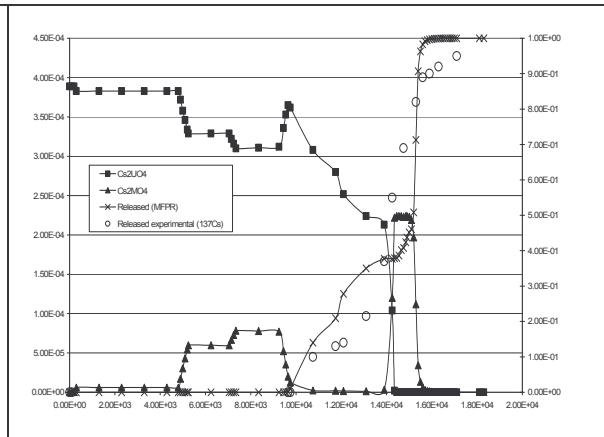


Fig. 11: Calculated Cs behaviour in VERCORS 5 as compared with experimental data (^{137}Cs) (Ducros 2001).

Similar good agreement is shown in Figures 12 and 13 for Mo and Ba behaviour in VERCORS 4 experiment. In Fig. 12 representing the evolution of the phase distribution and the release kinetics of molybdenum in VERCORS-4 test, it is seen that depending on the oxidation scenario, the molybdenum release occurs during a very short period of fuel oxidation. When steam is switched to hydrogen, the Mo release is terminated simultaneously with almost instantaneous and complete decomposition of the molybdenum-bearing components of the grey phase from which molybdenum is transferred to the metal phase.

The MFPR chemistry provides reasonable agreement with experimental data for the barium and strontium releases in the case of VERCORS-4 test including the high-temperature reducing phase. The predicted release of Ba as a function of time is shown in Fig. 13 along with the phase distribution. The release rate of Ba is calculated to be large during a short period at the beginning of the reducing stage of the test when the barium-bearing components of the grey phase are partially decomposed.



4. Conclusions

The new advanced mechanistic code MFPR for simulation of fission products release from irradiated UO_2 fuel is currently under development in collaboration between IRSN (Cadarache, France) and IBRAE (Moscow, Russia). The present paper includes main characteristics of the MFPR code, brief description of the new models and their validation against analytical tests and integral VERCORS experiments. The code is based on self-consistent consideration of evolution of various point defects (gas atoms, vacancies and interstitials) and extended defects (gas bubbles, dislocations, vacancy clusters and pores) and their mutual interactions under various irradiation and annealing regimes of UO_2 fuel operation. On this base, the new microscopic models for various physical processes related to the transport of fission products from UO_2 fuel were developed and validated against analytical tests. Results of this validation demonstrated significant improvement of the code predictions in comparison with previous codes and confirmed the enhanced predictive power of the advanced mechanistic approach.

In the field of chemically active elements, the mechanistic approach of MFPR is based on complex association of diffusion-vaporisation mechanism involving multiphase and multi-component equilibrium at grain boundary with accurate calculation of fuel oxidation. Examples of code application to VERCORS 4 and 5 experiments show the possibilities of the code in the frame of severe accident interpretation like PHEBUS experiments (Dubourg 2004).

Further development and validation of the MFPR code are foreseen in the field of increased association with fuel structure evolution, more accurate and exhaustive description of chemically active elements and application to LOCA and severe accidents interpretation.

5. Acknowledgements

Support and collaboration of Dr. P. Giordano (IRSN), Drs. V. Ozrin, V. Shestak and V. Tarasov (IBRAE) are highly appreciated.

6. References

- Berdyshev 2002 A.V. Berdyshev and M.S. Veshchunov, "Modelling of grain face diffusion transport and swelling in UO₂ fuel", Preprint IBRAE-2002-14, Moscow, 2002.
- Brailsford 1981 A.D. Brailsford, R. Bullough, *Philos. Trans. Royal. Soc. A* 302 (1981) 87.
- Cordfunke 1988 E.H.P.Cordfunke and R.J.M.Konings, *J. Nucl. Mater.* 152 (1988) 301-309.
- Cordfunke 1993 E.H.P.Cordfunke and R.J.M.Konings, *J. Nucl. Mater.* 201 (1993) 57-69.
- Dubourg 2003 R. Dubourg, G. Nicaise, "Development of mechanistic code MFPR for modeling fission product release from irradiated UO₂ fuel. Part2: Application to integral tests VERCORS 4/5 and PHEBUS FPT0/1," *Proc. Internat. Conference "TopFuel 2003: Nuclear Fuel for Today and Tomorrow. Experience and Outlook"*, Würzburg, Germany (March 16 to 19, 2003).
- Dubourg 2004 R.Dubourg, H.Manenc, G.Nicaise, M.Barrachin "FP release in the first two PHEBUS tests FPT0 and FPT1" submitted to *Nucl. Eng. Des.* (2004)
- Ducros 2001 G. Ducros, P.P.Malgouyres, M.Kissane, D.Boulaud, M.Durin, *Nucl. Eng. Des.*, 208 (2001) 191
- Evans 1997 J.H. Evans, *J. Nucl. Mater.* 246 (1997) 121.
- Geguzin 1971 Ya.E. Geguzin and M.A. Krivoglaz, "The Movement of Microscopic Inclusions in Solid State", *Metallurgiya*, Moscow, 1971, (in Russian).
- Grimmes 1991 R.W. Grimmes, C.R.A. Catlow, *Phil. Trans. R. Soc. London*, A335 (1991) 609 - 634.
- Heames 1992 T.J. Heames et al. "VICTORIA : A Mechanistic Model of Radionuclide Behavior in the Reactor Coolant System Under Severe Accident Conditions", NUREG/CR-5545 SAND90-0756 Rev 1 R3, R4, 1992.
- Hillert 1965 M. Hillert, *Acta Metall.* 36 (1965) 469.
- Imoto 1986 S. Imoto, *J. Nucl. Mater.* 140 (1986) 1927.
- Kashibe 1991 S. Kashibe, K. Une, *J. Nucl. Sci. Technol.* 28 (1991) 1090.
- Kashibe 1993 S. Kashibe, K. Une, *J. Nucl. Mater.* 206 (1993) 22.
- Kleykamp 1985 H. Kleykamp, *J. Nucl. Mater.*, 131 (1985) 221-246.

- Lindemer 1985 T.B. Lindemer and T.M. Besmann, J. Nucl. Matter. 130 (1985) 473-488.
- Mikhlin 1979 E.Ya. Mikhlin, J. Nucl. Mater. 87 (1979) 405.
- Moriyama 1997 K. Moriyama and H. Furuya, J. Nucl. Sci. and Techn. 34 (1997) 900–908.
- Nichols 1968 F.A. Nichols, J. Am. Ceram. Soc. 51 (1968) 468.
- Nogita 1994 K. Nogita and K. Une, Nuclear Instruments and Methods, **B91**, 301 (1994).
- Osborne 1992 M.F. Osborne and R.A. Lorenz, Nucl. Safety, 33 (1992) 344.
- Ozrin 2002 V.D. Ozrin, V.E. Shestak, V.I. Tarasov and M.S. Veshchunov, “Modelling of fission gas release during high-temperature annealing of irradiated UO₂ fuel”, Preprint IBRAE-2002-19, Moscow, 2002.
- Rest 1994 J. Rest, S.A. Zawadzki, "FASTGRASS, A Mechanistic Model for the Prediction of Xe, I, Cs, Te, Ba and Sr release from Nuclear Fuel under Normal and Severe-Accident Conditions", NUREG/CR-5840 TI92 040783, 1994.
- Shestak 2004 V.E. Shestak, V.I. Tarasov and M.S. Veshchunov, “Modelling of Defect Structure Evolution in Irradiated UO₂ Fuel in Framework of the MFPR Code”, Preprint IBRAE-2004-02, Moscow, Russia, 2004.
- Turnbull 1974 J.A. Turnbull, J. Nucl. Mater. 50 (1974) 62.
- Une 1990 K. Une, S. Kashibe, J. Nucl. Science and Technology, 27(11) (1990) 1002-10016.
- Veshchunov 2000 M.S. Veshchunov, J. Nucl. Mater. 227 (2000) 67–81.
- Veshchunov 2000a M.S. Veshchunov, A.V. Berdyshev, V.I. Tarasov, “Development of Fission Gas Bubble Models for UO₂ Fuel in Framework of MFPR Code”, Preprint IBRAE-2000-08, Moscow, 2000.
- Veshchunov 2002 M.S. Veshchunov and V.I. Tarasov, “Modelling of grain growth kinetics in irradiated and non-irradiated UO₂ fuel pellets in framework of the MFPR code”, Preprint IBRAE-2002-24, Moscow, Russia, 2002.
- Veshchunov 2003 M.S. Veshchunov, A.V. Berdyshev, V.D. Ozrin, V.E. Shestak, V.I. Tarasov, “Development of mechanistic code MFPR for modeling fission product release from irradiated UO₂ fuel. Part1: Development and validation of new models,” *Proc. Internat. Conference “TopFuel 2003: Nuclear Fuel for Today and Tomorrow. Experience and Outlook”*, Würzburg, Germany (March 16 to 19, 2003).
- Whapham 1966 A.D. Whapham, “Electron Microscope Observation of the Fission Gas Bubble Distribution in UO₂,” Nuclear Applications, 2 (1966) 123.
- Zacharie 1998 I. Zacharie, S. Lansart, P. Combette, M. Trotabas, M. Coster, M. Groos, J. Nucl. Mater. 255 (1998) 85-91.